



## Azacarbazole n-3 and n-6 polyunsaturated fatty acids ethyl esters nanoemulsion with enhanced efficacy against *Plasmodium falciparum*

Anna Jaromin<sup>a,\*</sup>, Silvia Parapini<sup>b</sup>, Nicoletta Basilio<sup>c</sup>, Magdalena Zaremba-Czogalla<sup>a</sup>, Agnieszka Lewińska<sup>d</sup>, Agnieszka Zagórska<sup>e</sup>, Maria Walczak<sup>f</sup>, Bożena Tyliśszczak<sup>g</sup>, Aleksandra Grzeszczak<sup>a</sup>, Marcin Łukaszewicz<sup>h</sup>, Łukasz Kaczmarek<sup>i</sup>, Jerzy Gubernator<sup>a</sup>

<sup>a</sup> Department of Lipids and Liposomes, Faculty of Biotechnology, University of Wrocław, Wrocław, Poland

<sup>b</sup> Dipartimento di Scienze Biomediche per la Salute, Università degli Studi di Milano, Milan, Italy

<sup>c</sup> Dipartimento di Scienze Biomediche, Chirurgiche e Odontoiatriche, Università degli Studi di Milano, Milan, Italy

<sup>d</sup> Faculty of Chemistry, University of Wrocław, Wrocław, Poland

<sup>e</sup> Department of Medicinal Chemistry, Jagiellonian University Medical College, Cracow, Poland

<sup>f</sup> Chair and Department of Toxicology, Jagiellonian University Medical College, Faculty of Pharmacy, Cracow, Poland

<sup>g</sup> Institute of Materials Science, Cracow University of Technology, Cracow, Poland

<sup>h</sup> Department of Biotransformation, Faculty of Biotechnology, University of Wrocław, Wrocław, Poland

<sup>i</sup> Pharmaceutical Research Institute, Warsaw, Poland

### ARTICLE INFO

#### Keywords:

Azacarbazoles

Flax oil

n-3 and n-6 polyunsaturated fatty acids ethyl esters

Nanoemulsion

*P. falciparum*

Malaria

### ABSTRACT

Alternative therapies are necessary for the treatment of malaria due to emerging drug resistance. However, many promising antimalarial compounds have poor water solubility and suffer from the lack of suitable delivery systems, which seriously limits their activity. To address this problem, we synthesized a series of azacarbazoles that were evaluated for antimalarial activity against D10 (chloroquine-sensitive) and W2 (chloroquine-resistant) strains of *P. falciparum*. The most active compound, 9*H*-3-azacarbazole (**3**), was encapsulated in a novel o/w nanoemulsion consisting of ethyl esters of polyunsaturated fatty acids n-3 and n-6 obtained from flax oil as the oil phase, S<sub>mix</sub> (Tween 80 and Transcutol HP) and water. This formulation was further analyzed using transmission electron microscopy, dynamic light scattering and *in vitro* and *in vivo* studies. It was shown that droplets of the **3**-loaded nanosystem were spherical, with satisfactory stability, without cytotoxicity towards fibroblasts and intestinal cell lines at concentrations corresponding to twice the IC<sub>50</sub> for *P. falciparum*. Moreover, the nanoemulsion with this type of oil phase was internalized by Caco-2 cells. Additionally, pharmacokinetics demonstrated rapid absorption of compound **3** (t<sub>max</sub> = 5.0 min) after intragastric administration of **3**-encapsulated nanoemulsion at a dose of 0.02 mg/kg in mice, with penetration of compound **3** to deep compartments. The **3**-encapsulated nanoemulsion was found to be 2.8 and 4.2 times more effective in inhibiting the D10 and W2 strains of the parasite, respectively, compared to non-encapsulated **3**. Our findings support a role for novel o/w nanoemulsions as delivery vehicles for antimalarial drugs.

### 1. Introduction

Malaria is a mosquito-borne infectious disease affecting mainly children and pregnant women from tropical countries. According to the World Health Organization (WHO), an estimated 228 million cases of malaria occurred worldwide in 2018, compared with 251 million cases

in 2010 and 231 million cases in 2017, indicating that some progress has been made in reducing global malaria cases. It is also reported that nineteen countries in sub-Saharan Africa and India carry almost 85% of the global malaria burden [1]. Unfortunately, a very disturbing fact is that current antimalarial drugs are rapidly losing their effectiveness due to rising parasite resistance [2]. This is exemplified by the emergence of

\* Corresponding author.

E-mail addresses: [anna.jaromin@uwr.edu.pl](mailto:anna.jaromin@uwr.edu.pl) (A. Jaromin), [silvia.parapini@unimi.it](mailto:silvia.parapini@unimi.it) (S. Parapini), [nicoletta.basilico@unimi.it](mailto:nicoletta.basilico@unimi.it) (N. Basilio), [magdalena.zaremba-czogalla@uwr.edu.pl](mailto:magdalena.zaremba-czogalla@uwr.edu.pl) (M. Zaremba-Czogalla), [agnieszka.lewinska@chem.uni.wroc.pl](mailto:agnieszka.lewinska@chem.uni.wroc.pl) (A. Lewińska), [agnieszka.zagorska@uj.edu.pl](mailto:agnieszka.zagorska@uj.edu.pl) (A. Zagórska), [maria.walczak@uj.edu.pl](mailto:maria.walczak@uj.edu.pl) (M. Walczak), [bozena.tyliszczak@pk.edu.pl](mailto:bozena.tyliszczak@pk.edu.pl) (B. Tyliśszczak), [aleksandra.grzeszczak@uwr.edu.pl](mailto:aleksandra.grzeszczak@uwr.edu.pl) (A. Grzeszczak), [marcin.lukaszewicz@uwr.edu.pl](mailto:marcin.lukaszewicz@uwr.edu.pl) (M. Łukaszewicz), [l.kaczmarek@ifarm.eu](mailto:l.kaczmarek@ifarm.eu) (Ł. Kaczmarek), [jerzy.gubernator@uwr.edu.pl](mailto:jerzy.gubernator@uwr.edu.pl) (J. Gubernator).

<https://doi.org/10.1016/j.bioactmat.2020.10.004>

Received 29 May 2020; Received in revised form 27 September 2020; Accepted 7 October 2020

Available online 24 October 2020

2452-199X/© 2020 The Authors. Production and hosting by Elsevier B.V. on behalf of KeAi Communications Co., Ltd. This is an open access article under the CC

BY-NC-ND license (<http://creativecommons.org/licenses/by-nc-nd/4.0/>).

chloroquine (CQ)-resistant *P. falciparum* parasites about a decade following the widespread introduction of the highly cost-effective treatment involving CQ [3]. Furthermore, not only CQ-resistant strains have spread around the world, but they are evolving. Resistance of *P. falciparum* to the currently used artemisinin-based chemotherapeutics is the next urgent problem that needs to be addressed [4,5]. In 2009, *P. falciparum* strains resistant to artemisinin were first identified in western Cambodia [6] with later occurrences in other parts of Southeast Asia [7].

This requires an immediate need for the discovery and development of next-generation therapeutics and novel compounds characterized by high selectivity and effectiveness [8,9]. Unfortunately, many of the newly emerging drug candidates are excluded due to low solubility, which is a limiting requirement for initial *in vitro* activity evaluation against *Plasmodium*. However, some of these new chemical agents are active after encapsulation in nanocarriers. Thus, the development of nanotechnology-based drug delivery systems appears to be a very attractive strategy to combat malaria. Use of nanomedicine brings many benefits, such as lowering the progression of resistance, reducing drug toxicity, controlled release, increased bioavailability and the selectivity of drugs, contributing to the overall diagnosis, control and treatment of malaria by targeted delivery [10–12]. Several lipid-based delivery systems, such as liposomes [13–15], solid lipid nanoparticles [16,17] and micro- and nanoemulsions, as well as self-emulsifying drug delivery systems [18–20] have already proved their effectiveness in malaria therapy.

Oil-in-water (o/w) nanoemulsions are systems composed of oil, surfactants and co-surfactants dispersed in an aqueous phase. Nanoemulsion droplet sizes fall typically in the range of 20–200 nm and show narrow size distributions [21]. The great advantage of this type of carrier is the possibility to encapsulate and deliver hydrophobic agents, or molecules that are significantly more toxic in the free form. Nowadays, the FDA (U.S. Food and Drug Administration) has approved for clinical use several nanoemulsion formulations of drugs characterized by poor water solubility, such as cyclosporin (Neoral®) and ritonavir (Norvir®) [22]. There are also many successful examples of incorporation of antimalarials in nanoemulsion systems. Primaquine encapsulated in an oral lipid nanoemulsion in the 10–200 nm size range showed effective antimalarial activity against *Plasmodium berghei* infection in mice at a 25% lower dose in comparison to conventional oral dosing [23]. Another interesting approach was presented in a study by Laxmi et al. which proved that the absorption of artemether from a nanoemulsion resulted in a 2.6-fold increase in bioavailability, as compared to administration of the free drug [24]. In turn, research performed by Borhade et al. revealed that mice treated with 10 mg/kg clotrimazole nanoemulsion showed the highest suppression of parasitemia, and parasitemia was significantly lower than that observed after treatment of clotrimazole suspension at 10 mg/kg. Moreover, survival of mice treated with this nanosystem was significantly prolonged in comparison to treatment of the free drug in suspension at the same doses [25].

This encouraged us to develop a new nanoemulsion system dedicated for delivery of azacarbazoles, derivatives of carbazole. Carbazole (9H-carbazole) is a heterocyclic tricyclic molecule, consisting of two six-membered benzene rings fused on either side of a five-membered

nitrogen-containing ring (pyrrole)(Fig. 1).

This skeleton is present in many biologically active compounds [26–28]. One of the most important properties of the carbazole-core agent is antiplasmodial activity [29–31]. Many recently published reports confirmed also that carbazole-based compounds exert promising antibacterial [32], antiviral [33], antifungal [34] and antiparasite [35] activities. Several authors emphasize simultaneously its potential use for the treatment of neurological disorders [36–39], or cancer [40,41]. More importantly, the carbazole scaffold is also found in marketed drugs, such as Carvedilol and Carprofen.

Thus, the aim of this study was the development of a novel o/w nanoemulsion (NE) system for the most active, compound but with limited solubility in water, namely **3** (9H-3-azacarbazol) among the 12 synthesized azacarbazoles tested against CQ-sensitive (D10) and CQ-resistant (W2) strains of *P. falciparum*. For this purpose, we selected a concentrated form of ethyl esters of n-3 and n-6 polyunsaturated fatty acids, obtained in the process of flax oil biotransformation, as an oil phase of the designed nanocarrier. These compounds were isolated from flax oil and subsequently transesterified from the triacylglycerol to the ethanol form. Therefore, they meet the definition of a nutraceutical, i.e. a product which is a concentrate of bioactive ingredients isolated from plants. The obtained nanoemulsions were further characterized as well as evaluated in *in vitro* and *in vivo* studies. Finally, both unloaded as well as **3** loaded nanoemulsions (3-NE) were tested to verify the efficacy of the nanoencapsulation approach against *P. falciparum* strains. Literature reviews have so far revealed no studies on the application of an o/w nanoemulsion as a delivery system for this type of azacarbazol, nor of the use of ethyl esters of polyunsaturated fatty acids for the preparation of nanocarriers of antimalarials.

## 2. Experimental section

### 2.1. Materials and methods

#### 2.1.1. Materials

Azacarbazoles were synthesized using methods reported previously, namely **1** (9H-1-azacarbazole) [42], **2** (9H-2-azacarbazole) [43], **3** (9H-3-azacarbazole) [44], **4** (8-methyl-9H-1-azacarbazole) [45], **5** (6-methyl-9H-1-azacarbazole) [46], **6** (1,4-dimethyl-1H-1-azacarbazole) [47], **7** (9H-1,8-diazacarbazole) and **8** (9H-2,7-diazacarbazole) [48], **9** (9H-1,5-diazacarbazole) [data not published], **10** (9H-4,5-diazacarbazole) [48], **11** (1-methyl-1H-1,8-diazacarbazole) and **12** (4-methyl-4H-4,5-diazacarbazole) [49]. Diethylene glycol monoethyl ether (Transcutol HP) was a gift from Gattefossé (Saint Priest, France). Concentrated forms of the ethyl esters of polyunsaturated fatty acids n-3 and n-6, containing about 67% polyunsaturated fatty acids from the n-3 and n-6 families, was produced by LeenLife Pharma (Kraków, Poland). Tween 80, DMSO, fetal bovine serum (FBS), bovine trypsin, hemin (Ferroprotoporphyrin IX chloride, FP), chloroquine diphosphate, DAPI (4',6-diamidino-2-phenylindole), Nile Red and MTT (3-[4,5-dimethylthiazol-2-yl] –2,5-diphenyltetrazolium bromide) were purchased from Sigma-Aldrich (Poznan, Poland). GlutaMAX™ (L-glutamine) was from Life Technologies (Warsaw, Poland) and Antibiotic-Antimycotic 100x from Biowest (Zgierz, Poland). The normal human dermal fibroblast cell line (NHDF), Non-Essential Amino Acid Solution (100x) and Minimum Essential Medium Eagle Alpha Modifications medium were purchased from Lonza (Warsaw, Poland). The Caco-2 cell line was a kind gift from Prof. Piotr Dziegiel, Department of Histology and Embryology, Wrocław Medical University, Poland. Dako Fluorescent Mounting Medium was from DAKO (Konin, Poland). AlbuMax and RPMI 1640 were obtained from Invitrogen (Milan, Italy) and EuroClone (Celbio Milan, Italy), respectively. All chemicals and reagents not specified in the text were of analytical grade and used without further purification.

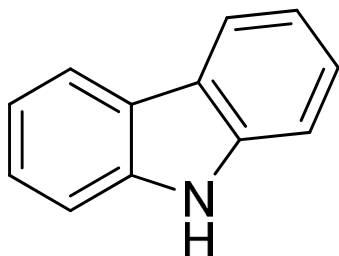


Fig. 1. Chemical structure of carbazole.

## 2.2. *P. falciparum* cultures and drug susceptibility assay

*P. falciparum* cultures were established according to Trager and Jensen, with slight modifications [50]. The CQ-susceptible strain D10 and the CQ-resistant strain W2 were maintained at 5% hematocrit in RPMI medium with the addition of 1.0% AlbuMax, 0.01% hypoxanthine, 20 mM HEPES, and 2 mM glutamine. All cultures were maintained at 37 °C in a standard gas mixture consisting of 1% O<sub>2</sub>, 5% CO<sub>2</sub>, and 94% N<sub>2</sub>. Samples (compounds dissolved in DMSO, unloaded and 3-loaded (2.0 mg/ml) coarse o/w emulsions) were placed in 96-well flat-bottomed microplates and serial dilutions were prepared. Asynchronous cultures with parasitaemia of 1.0–1.5% and 1.0% final hematocrit were aliquoted into the plates and incubated for 72 h at 37 °C. Parasite growth was determined spectrophotometrically (OD<sub>650</sub>) by measuring the activity of parasite lactate dehydrogenase (pLDH), according to a modified version of the method of Makler [51]. The anti-malarial activity was expressed as 50% inhibitory concentrations (IC<sub>50</sub>); each IC<sub>50</sub> value is the mean and standard deviation of at least three separate experiments performed in duplicate.

## 2.3. The cytotoxic activity test

NHDF cells were cultured in alpha-MEM medium supplemented with 10% heat-inactivated FBS, GlutaMAX™ and antibiotics. Caco-2 cells were grown in Dulbecco's modified Eagle's medium (DMEM) medium containing 20% FBS, 1% non-essential amino acids, GlutaMAX™ and antibiotics. Cell viability was determined as previously described [52] using the MTT assay [53]. Different doses of 2, 3, 6, 12 dissolved in DMSO, CQ (in water) as well as unloaded and 3-loaded (2.0 mg/ml) coarse o/w emulsions were added to each well, mixed and incubated for 24 or 48 h. Results were expressed as IC<sub>50</sub> values, or as the percentage of survival cells with respect to the control (not treated cells).

## 2.4. Calculation of log D and log P<sub>o/w</sub>

The distribution coefficient (log D) was calculated using the MarvinSketch software (version 19.26.0, ChemAxon Ltd.), whereas the partition coefficient between *n*-octanol and water (log P<sub>o/w</sub>) was calculated using the SwissADME web tool [54] and was expressed as an average of iLOGP, XLOGP3, WLOGP, MLOGP and SILICOS-IT predictions.

## 2.5. Hemolytic activity

The experiments were carried out according to a procedure described previously [55]. The hemolytic effect was determined on the basis of hemoglobin released from human erythrocytes (5% hematocrit) after incubation in PBS containing 5 mM glucose (2 h, 37 °C) with 2, 3, 6, 12 and CQ (final concentration 50 and 100 μM, respectively) alone, or in the presence of 10 μM FP. After incubation, samples were centrifuged and the absorbance of supernatants was measured at 412 nm. Hemolysis (H) was calculated according to the following formula [56]:

$$H (\%) = \frac{(A_{\text{sample}} - A_{\text{negative control}})}{(A_{\text{positive control}} - A_{\text{negative control}})} \times 100 \quad (1)$$

where  $A_{\text{sample}}$ ,  $A_{\text{negative control}}$ , and  $A_{\text{positive control}}$  represent the absorbances of the sample, and negative (mechanical hemolysis, erythrocytes in PBS buffer) and positive (erythrocytes in distilled water) controls, respectively. The study was approved by the Bioethics Commission at the Lower Silesian Medical Chamber (1/PNHAB/2018).

## 2.6. Preparation of o/w emulsion

The first stage involved construction of a pseudoternary phase diagram [57]. Ethyl esters of n-3 and n-6 polyunsaturated fatty acids,

Tween 80 and Transcutol HP were used as the oil phase, surfactant and cosurfactant, respectively. Distilled water was selected as an aqueous phase. Surfactant and cosurfactant ( $S_{\text{mix}}$ ) were mixed in a 1:1 wt ratio. Oil phase and  $S_{\text{mix}}$  were combined in different weight ratios in different glass vials to delineate the boundaries of phases. An aqueous titration method was used for the construction of the pseudoternary phase diagram, which involved the stepwise addition of water to each vial, and then mixing the components with the help of a vortex mixer. The o/w emulsion phase was identified as the region in the phase diagram where milky, easily flowable formulations were obtained, based on visual observation. The following composition was selected for further studies: 5% w/w of oil phase, 10% w/w of  $S_{\text{mix}}$  and 85% w/w of water. To obtain a 3-loaded o/w emulsion, an appropriate amount of 3 was dissolved in a mixture of oil phase and  $S_{\text{mix}}$ .

## 2.7. Preparation of nanoemulsion

To prepare o/w nanoemulsion (NE), a milky o/w emulsion with a composition of 5% w/w of oil phase, 10% w/w of  $S_{\text{mix}}$  (1:1 w/w) and 85% w/w of water, was immediately diluted with water (1:100 v/v). To prepare 3-NE, 3-loaded (2.0 mg/ml) o/w emulsion was diluted in the same proportion. The Nile Red loaded NE was prepared with a saturated Nile Red solution in the oil phase and diluted in the same way.

## 2.8. Particle shape and morphology analyses

Transmission Electron Microscopy (TEM) was used to study the shape and morphology of the coarse o/w emulsions as well as NE. Each sample was first diluted, then spotted on a grid and stained with 2% uranyl acetate. The samples were observed with an FEI Tecnai G2 20 XTWIN transmission electron microscope (FEI, Hillsboro, USA).

## 2.9. Size and Zeta potential analysis

The mean droplet size and Zeta potential of the NE and 3-NE were measured using a Zetasizer Nano-ZS (Malvern Instruments Ltd., Malvern, UK). The polydispersity index (PdI) was obtained using the instrument's built-in software.

## 2.10. Stability of nanoemulsion

The average size and PdI of NE and 3-NE were measured just after preparation and, additionally, after storage at 4 °C for 7, 14, 21, 28 and 152 days.

## 2.11. In vitro uptake study

Caco-2 cells were grown in DMEM culture medium containing 20% FBS, 1% non-essential amino acids, GlutaMAX™ in a humidified 5% CO<sub>2</sub>/95% air atmosphere at 37 °C. For experiments, cells were seeded onto glass cover slides, placed in 24-well culture plates. After 48 h incubation, upon reaching around 90% confluence cells were treated with Nile Red loaded NE, fixed and stained with DAPI as described earlier [58]. Slides were analyzed by using a Leica TCS SP8 confocal microscope (Leica-Microsystems, Mannheim, Germany) with HC PL APO CS2 63x/1.40 oil objective. Nile Red and DAPI were excited with an argon laser at 488 nm and a 405 nm laser, respectively.

## 2.12. In vivo pharmacokinetic evaluation

### 2.12.1. Animals

An experimental group of 48 adult male mice (CD-1, 18–21 g) were used in the study. The animals were purchased from the Animal House at the Faculty of Pharmacy, Jagiellonian University Medical College, Krakow, Poland. During the habituation period, mice were divided into groups of 6 individuals and kept in plastic cages (252 mm × 167 cm ×

140 cm) at a controlled room temperature ( $22 \pm 2$  °C), humidity ( $55 \pm 10\%$ ), full spectrum cold white light (350–400 lx), on 12 h light/dark cycles (the lights on at 7:00 a.m., and off at 19:00 p.m.), and had free access to standard laboratory pellet and tap water. For the pharmacokinetic study, compound **3**, in the form of 3-NE (0.02 mg/ml), was administered by an intragastric (i.g.) gavage at a dose of 0.02 mg/kg. Blood samples ca. 1 ml were collected at 0 min (predose), 5 min, 15 min, 30 min, 60 min, 120 min, 240 min and 480 min after compound **3** administration. For each time point, 6 mice were sampled. The blood samples were collected under general anesthesia induced by *i.p.* injections of 50 mg/kg ketamine plus 8 mg/kg xylazine. The blood samples were taken into heparinized tubes, immediately centrifuged at 3500 rpm for 10 min and plasma was collected. The plasma samples were immediately frozen at  $-80$  °C for LC/ESI-MS/MS analysis. All experimental procedures were carried out in accordance with EU Directive 2010/63/EU [59] and approved by the 1st Local Ethics Committee for Experiments on Animals of the Jagiellonian University in Krakow, Poland.

### 2.12.2. Pharmacokinetic study

Pharmacokinetic parameters were calculated by a non-compartmental approach [60] from the average concentration values, using Phoenix WinNonlin software (Certara, Princeton, NJ 08540 USA). The first order elimination rate constant ( $\lambda_z$ ) was calculated by linear regression of time versus log concentration. Next, the area under the mean serum concentration versus time curve ( $AUC_{0 \rightarrow t}$ ) was estimated using the log-linear trapezoidal rule (Eq. (2)), where  $C_i$  is the concentration of the compound, and  $t_i$  is the time of sampling.

$$AUC_{0 \rightarrow t} = \sum_{i=1}^n ((C_i + C_{i+1}) / 2) \cdot (t_{i+1} - t_i) \quad (2)$$

Area under the first-moment curve ( $AUMC_{0 \rightarrow t}$ ) was estimated by calculation of the total area under the first-moment curve using equation (3):

$$AUMC_{0 \rightarrow t} = \sum_{i=1}^n ((t_i \cdot C_i + t_{i+1} \cdot C_{i+1}) / 2) \cdot (t_{i+1} - t_i) \quad (3)$$

Mean residence time (MRT) was calculated as:

$$MRT = \frac{AUMC_{0 \rightarrow t}}{AUC_{0 \rightarrow t}} \quad (4)$$

Total clearance ( $Cl_T$ ) was calculated as:

$$Cl_T = \frac{F \cdot D_{i.g.}}{AUC_{0 \rightarrow t}} \quad (5)$$

Volume of distribution ( $V_d$ ) was calculated as:

$$V_d = \frac{F \cdot D_{i.g.}}{\lambda_z \cdot AUC_{0 \rightarrow t}} \quad (6)$$

where  $D_{i.g.}$  is an intragastric dose of compound **3**.

### 2.12.3. Analytical method

Concentration of **3** in plasma was determined by an LC/ESI-MS/MS technique using a TSQ Quantum mass spectrometer (Thermo Scientific, Waltham, MA, USA) coupled to a UHPLC UltiMate 3000 (Dionex, Sunnyvale, CA, USA). Chromatography separation was achieved with an AquityC18 BEH  $3.0 \times 100$  mm,  $1.7 \mu\text{m}$  analytical column (Waters, Milford, MA, USA) using acetonitrile and water as a mobile phase, with addition of 0.1% (v/v) formic acid under isocratic conditions (60:40 v/v) at a flow rate of 0.4 ml/min. Quantification of compound **3** and 2-(4-methyl-1-piperazinyl)-4-phenylquinazoline, used as an internal standard (IS), was performed using a positive ionisation SRM mode, monitoring ion transitions  $m/z$  169.1  $\rightarrow$  115.1 for compound **3** and  $m/z$  305  $\rightarrow$  248 for IS. The working parameters of the mass spectrometer were as follows: spray voltage: 4000V, vaporiser temperature: 300 °C; sheath

gas pressure: 20 arb.; auxiliary gas pressure: 15 arb.; capillary temperature: 350 °C, collision pressure: 1.5 mTorr.

### 2.12.4. Standard solutions preparation

An amount of 1 mg of **3** was accurately weighed and transferred into a 1 ml volumetric flask using methanol. Further dilutions were performed in the same solvent to prepare working standard solutions of the analyte at the following concentrations: 0.25, 0.5, 1.0, 5.0, 10, 50, 100, 250, 500 and 1000 ng/mL, for calibration curve samples. To prepare samples for the calibration curve, plasma was spiked with 5  $\mu\text{l}$  of IS, obtaining the final concentration of 50 ng/ml and 5  $\mu\text{l}$  of standards working solutions at the required concentrations for the calibration curve. After addition of the standard solutions, samples were mixed and purified.

### 2.12.5. Sample preparation

A 50  $\mu\text{l}$  sample volume of plasma was transferred into an Eppendorf tube and spiked with 5  $\mu\text{l}$  of IS solution (250 ng/ml), giving a final concentration of 50 ng/ml. After 5 min of mixing (1500 rpm), the samples were incubated at 4 °C for 10 min. Proteins were precipitated using 200  $\mu\text{l}$  acetonitrile after 10 min of samples shaking (1500 rpm). Finally, samples were centrifuged (10 000 rpm, 10 min, 4 °C) and the supernatant was transferred into a chromatographic vial for LC/ESI-MS/MS analysis.

### 2.13. Statistical analysis

All data are expressed as the mean  $\pm$  standard deviation of at least three measurements. Statistical analyses were performed with GraphPad Prism software using One-way ANOVA, followed by Dunnett's multiple comparisons test. Probability values  $p < 0.05$  were considered statistically significant. The Dunnett's test compares two or more experimental groups against a single control group.

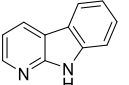
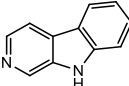
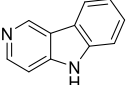
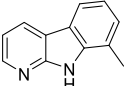
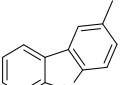
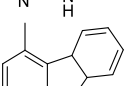
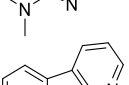
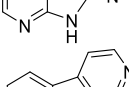
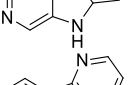
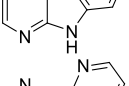
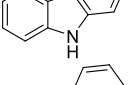
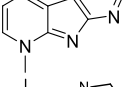
## 3. Results and discussion

The twelve synthesized azacarbazoles, as well as a well-known antimalarial drug, CQ, were screened *in vitro* for inhibitory activity against the CQ-sensitive D10 and CQ-resistant W2 strains of *P. falciparum*. Four compounds (**2**, **3**, **6** and **12**) from the group of 12 compounds synthesized displayed a range of  $IC_{50}$  values from 1954.6 to 4419.3 ng/ml, whereas the rest showed no effects below 5000 ng/ml (Table 1). According to the activity criteria, if the  $IC_{50}$  is  $> 5 \mu\text{g/ml}$ , the compound is classified as inactive, whereas, if the  $IC_{50}$  is between 0.5 and  $5 \mu\text{g/ml}$ , the compound is classified as moderately active and, if the  $IC_{50}$  is  $< 0.5 \mu\text{g/ml}$ , the compound is classified as active [61]. Therefore, on the basis of this ranking, we can conclude that these four derivatives exhibited moderate activity, whereas the remaining compounds demonstrated no activity towards the tested strains. It is worth noting that, although the obtained values are higher than for CQ, the active chemicals have resistance indexes (RI)  $\leq 1.3$ , suggesting no cross resistance with CQ.

In the context of our research, we were also interested in evaluating the degree of selectivity of the synthesized compounds towards the malaria parasite by conducting cytotoxicity studies on a normal human dermal fibroblast cell line. Together with antiprotozoal activity, a promising antimalarial agent should not exert toxicity against host cells and selectivity, expressed as SI values (See Table 1), should be high. It is worth mentioning that compounds having an SI  $< 2.0$  generally show strong antimalarial activity, but are usually accompanied by toxicity and are, therefore, not suited as antimalarials. Three of the compounds tested (**2**, **3** and **12**) have both selectivity indexes  $> 10$ , indicating low cytotoxicity and good selectivity for *P. falciparum*. In other words, the cytotoxicity of **2** and **3** as well as **12** towards normal human dermal fibroblast cells occurs at much higher concentrations than in the case of *P. falciparum*. Interestingly, **6**, which showed the weakest antiplasmodial

**Table 1**

*In vitro* antimalarial activity of azacarbazoles against the D10 (CQ-sensitive) and W2 (CQ-resistant) strains of *P. falciparum*, cytotoxicity on NHDF cells and log  $P_{o/w}$  and log  $D$ .

Compound	Structure	log $P_{o/w}^a$	log $D^b$			<i>P. falciparum</i> IC <sub>50</sub> (ng/ml)		RI <sup>c</sup>	Cytotoxicity <sup>d</sup> IC <sub>50</sub> (ng/ml)	SI <sub>D10</sub> <sup>e</sup>	SI <sub>W2</sub> <sup>f</sup>
			pH 7.4	pH 7.2	pH 5.5	D10	W2				
1		2.53	2.24	2.24	2.24	>5000	>5000	–	–	–	–
2		1.61	1.87	1.87	1.69	3329.7 ± 741.9	3669.9 ± 707.6	1.1	39950.0 ± 1105.3	12.0	10.9
3		2.22	1.26	1.17	0.90	1954.6 ± 263.0	2221.0 ± 752.0	1.1	32043.3 ± 1429.5	16.4	14.4
4		2.01	2.75	2.75	2.75	>5000	>5000	–	–	–	–
5		2.81	2.75	2.75	2.75	>5000	>5000	–	–	–	–
6		2.79	1.27	1.23	0.09	4419.3 ± 458.4	4183.1 ± 1041.5	0.9	11753.3 ± 143.6	2.6	2.8
7		1.87	1.39	1.39	1.39	>5000	>5000	–	–	–	–
8		1.49	0.65	0.64	0.30	>5000	>5000	–	–	–	–
9		1.82	1.41	1.41	1.41	>5000	>5000	–	–	–	–
10		1.63	1.42	1.42	1.43	>5000	>5000	–	–	–	–
11		1.92	1.93	1.93	1.93	>5000	>5000	–	–	–	–
12		1.66	2.01	2.01	2.01	3163.6 ± 621.4	3993.4 ± 269.3	1.3	42830.0 ± 3312.8	13.5	10.7
CQ*		–	0.88	0.64	–0.76	18.4 ± 8	262.3 ± 102.0	14.2	21126.7 ± 1179.8	1148.2	80.5

<sup>a</sup> The predictions were performed using the SwissADME tool and MarvinSketch software<sup>b</sup>, \* CQ phosphate, log  $D_2$ ; <sup>c</sup> Ratios between the IC<sub>50</sub> values of each compound against W2 and D10 strains of *P. falciparum*, <sup>d</sup> The cytotoxic activity assayed *in vitro* on NHDF cells using the MTT assay, <sup>e</sup> SI<sub>D10</sub> = IC<sub>50</sub>(NHDF)/IC<sub>50</sub>(D10), <sup>f</sup> SI<sub>W2</sub> = IC<sub>50</sub>(NHDF)/IC<sub>50</sub>(W2).

activity, was also the least selective, whereas **3** was the most promising compound, as evidenced by the lowest IC<sub>50</sub> and high SI values. There was also no direct correlation between the structures of the compounds, their hydrophobicity (expressed as log  $P_{o/w}$ ) and biological activities.

These observations inspired us to establish the ionic forms present at pH 7.4 (blood), 7.2 (cytoplasm), and 5.5 (*P. falciparum* food vacuole (FV)) of the studied compounds. The distribution coefficient (log  $D$ ) values at representative pH values for blood, cytoplasm, and FV were calculated, in order to explore the role of a possible accumulation of azacarbazoles in the FV on antimalarial activity (Table 1). The distribution coefficient is an expression of the lipophilicity of compounds

which reflects the equilibria of ionic forms (unionized and ionized) at a given pH. Most drugs have ionisable groups. Thus, log  $D$  is a better descriptor than log  $P$  that reflects the partitioning of a mixture of drug species as well as the actual drug lipophilicity at any given pH. Moreover, it is generally accepted that compounds with a log  $D$  from 0 to 3 have a good balance between solubility and permeability and exhibit good chemical characteristics required for cell membrane permeation. The major function of FV is the degradation of host haemoglobin via a series of peptidases during the erythrocytic life stages of the parasite. *Plasmodium* parasites polymerise ferriprotoporphyrin IX to crystalline haemozoin that becomes a distinct feature of the FV of trophozoite and

schizont parasites [62–64]. Several anti-malarial drugs kill the parasite by interfering with its metabolic pathway and FP polymerisation is the main target. Chloroquine accumulates in the FV and, once there, inhibits polymerisation either by binding free FP, or by capping FP polymers, which results in the accumulation of unpolymerised FP and FP-CQ complexes which are toxic for the parasites [65,66]. Only a neutral form of CQ can diffuse across the FV membrane where, in the acidic environment of the FV, it is protonated and is subsequently unable to freely diffuse out of the FV again. Thus, according to the data reported in Table 1, compounds 3 and 6 exhibited the most favourable log *D* parameters (compared to CQ), and characteristics that would favor accumulation in the FV of the parasite.

Based on the above results, only compounds manifesting antiplasmodial activity were selected for further investigations. Having proven that azacarbazoles are not toxic for normal human fibroblasts, we decided to use hemolysis, characterized by erythrocyte rupture, as an additional method for cytotoxicity evaluation, and follow the release of hemoglobin. It is well known that the presence of extracellular hemoglobin accompanies acute and chronic vascular disease, inflammation, thrombosis, and renal impairment [67]. Unfortunately, some antimalarials, e.g. artemisinin derivatives, can cause hemolysis and an increasing number of studies report acute haemolytic anaemia following their use [68]. The compounds tested in our study (2, 3, 6 and 12) were evaluated at two concentrations each, namely 50 and 100  $\mu\text{M}$ , corresponding to approximately two-fold and four-fold their respective  $\text{IC}_{50}$  values against *P. falciparum* (Fig. 2a). None of the examined agents caused significant lysis of human erythrocytes at the concentrations tested, which confirms a lack of toxicity towards mammalian cells.

We then extended our experiment and tested the percentage of hemolysis under conditions mimicking severe malaria. For this purpose, incubation of 2, 3, 6, 12 and CQ with erythrocytes in the presence of 10  $\mu\text{M}$  of FP was performed, as such levels of heme can be found in the course of this disease [69]. It is clearly seen that the occurrence of 2, 3, 6 and CQ-FP complexes drastically increased the percentage of hemolysis (Fig. 2b). On the other hand, the trend observed for CQ showing the highest degree of hemolysis at 50  $\mu\text{M}$ , is consistent with the results published by Omodeo-Salè *et al.* [55], although the measured lysis level is higher in our study. The effect of azacarbazoles, similar to CQ, manifested by an increase in heme-induced human erythrocyte lysis, could be associated with the enhanced ability of heme from 2, 3, and 6-FP complexes to intercalate between phospholipids within the erythrocyte membrane [70,71]. Additionally, interactions of compounds with the porphyrin ring of heme to varying degrees, as well as different hydrophobicity and the molecular sizes of formed complexes, should be considered as factors influencing the observed phenomenon. Surprisingly, both 6-FP and 12-FP at 50  $\mu\text{M}$  and 12-FP also at 100  $\mu\text{M}$ , were less hemolytic than CQ-FP complexes at similar concentrations, confirming the safety and lack of toxicity associated with these two compounds. Also, a lack of direct correlation between hemolytic activity and anti-malarial activity, as described for other groups of compounds [72], is

observed, suggesting that the mechanism of antiplasmodial action is complex, and is probably not limited only to the effects at the level of erythrocyte membranes.

Although the modes of action of the azacarbazoles described in this study remain to be elucidated, we decided to conduct encapsulation studies of one of the compounds, namely compound 3, in a nanosystem to estimate its antimalarial potential in such a delivery form. The choice to encapsulate 3, despite the promising hemolytic properties of 12, was driven by the fact that it was the most active and selective agent against *P. falciparum* in the series of compounds synthesized.

Since the oral route is usually the first choice for clinically uncomplicated malaria, we therefore focused only on components used in oral administration to develop the nanocarrier. The oil phase consisted of a concentrated form of ethyl esters of polyunsaturated fatty acids n-3 and n-6. These are examples of nutraceuticals, as well as dietary supplements and functional foods exhibiting pro-health properties. Further, Tween 80 was used as a nonionic surfactant, due to its high solubilization properties as well as biocompatibility and lack of toxicity [73]. Finally, Transcutol HP, a hydrophilic cosurfactant was applied because of proven activity as a solubilizer for solubility and bioavailability enhancement of drug delivery via oral routes, as well as being safe [74].

Through the use of ethyl esters as oil phase and Tween 80 and Transcutol HP as a surfactant and cosurfactant mixture ( $S_{\text{mix}}$ ), at a ratio of 1:1 (w/w), a pseudoternary phase diagram was constructed using the water titration method, with the aim of determining the concentration range of constituents necessary for the production of a milky o/w emulsion (Fig. 3a). By analyzing the resulting phase diagram, we concluded that emulsion is formed when the water phase is at least 60%. This phenomenon is a consequence of a reduction of the interfacial tension, leading to growing fluidity of the interface and an increase in the entropy of the system. Additionally, it has been proposed that there is intensified penetration of the ethyl esters in the hydrophobic region of the surfactant monomers [75]. Another interesting observation is that the emulsion was created only at the water-rich apex of the phase diagram, constituting proof that an o/w emulsion has been produced. With the knowledge that instability is a common problem with o/w emulsions, we used a crash dilution method [76] to dilute the milky emulsion, in this way, leading to the creation of an opalescent nanoemulsion (Fig. 3b). Based on the results of the optimization studies conducted for this process, we selected one model composition of o/w emulsion for dilution purposes, namely, 5% w/w of oil phase, 10% w/w of  $S_{\text{mix}}$  and 85% w/w of water, for further characterization. As can be seen in the TEM images, both o/w emulsion and nanoemulsion formed after dilution in water in a ratio of 1: 100 v/v have a spherical shape (Fig. 3c and d).

The potential of 3 to be encapsulated in NE was further evaluated with respect to size, Zeta potential, stability and toxicity to human cells. Both unloaded (NE) and 3-loaded nanoemulsion 3-NE (0.02 mg/ml) have droplets in the nano-range. The presence of encapsulated 3 results in a slightly smaller size (117.70 nm) compared to the unloaded carrier

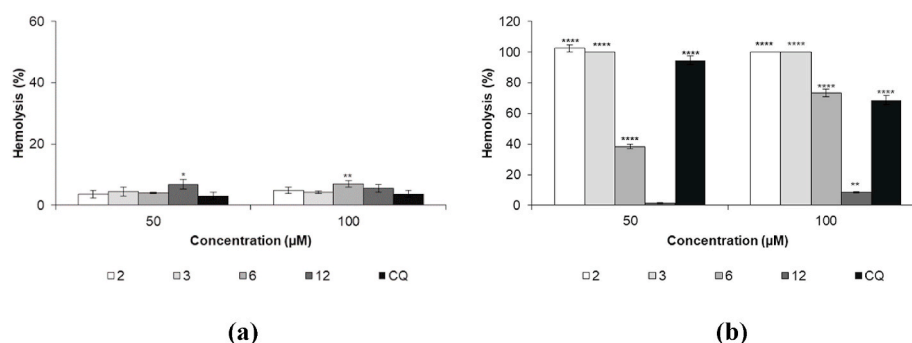
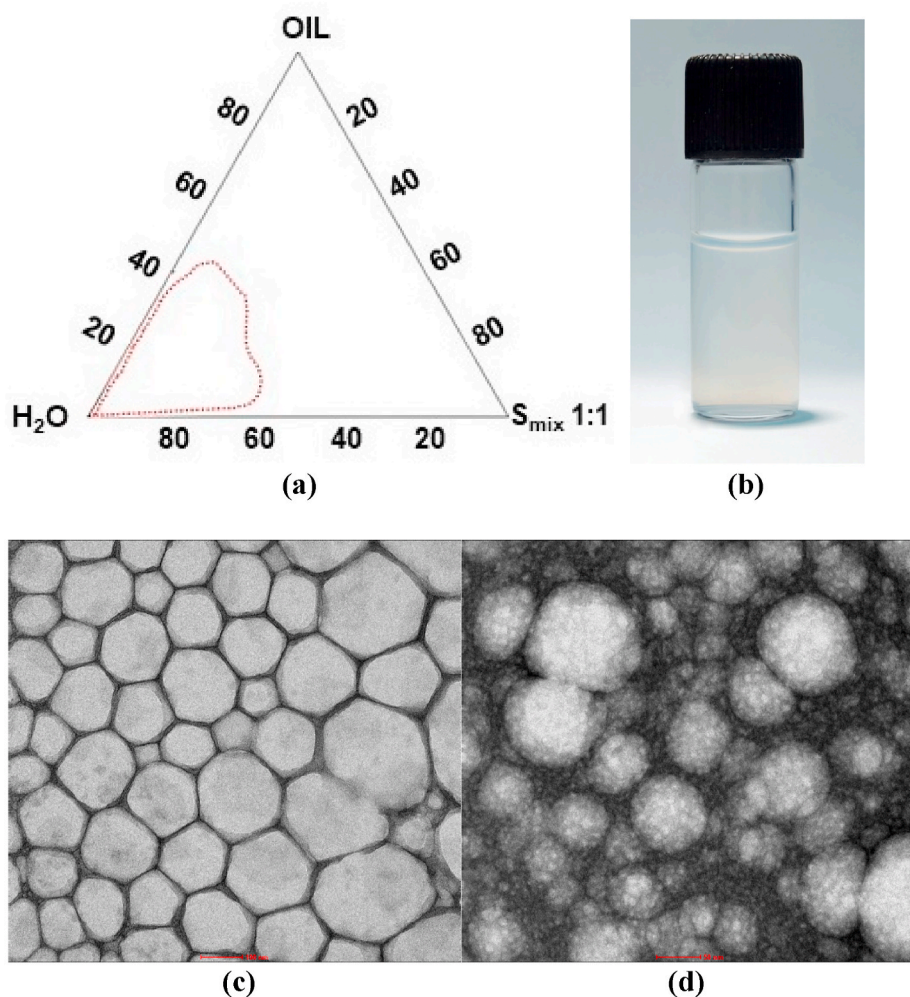


Fig. 2. Hemolysis of human erythrocytes induced by 2, 3, 6, 12 and CQ without FP (a) and in the presence of 10  $\mu\text{M}$  FP (b). \* show the statistical significance (\* $p$  < 0.05, \*\* $p$  < 0.01 and \*\*\*\* $p$  < 0.0001) as compared to control (mechanical hemolysis), calculated by using One-way ANOVA.



**Fig. 3.** Pseudoternary phase diagram composed of ethyl esters as the oil phase, Tween 80 and Transcutol HP as a surfactant and cosurfactant mixture ( $S_{mix}$ ) at a ratio of 1:1 (w/w) and water; marked area represents the o/w emulsion (a). Visual appearance of nanoemulsion formed after dilution of o/w emulsion (5% w/w of oil phase, 10% w/w of  $S_{mix}$  and 85% w/w of water) in water in a ratio of 1: 100 v/v (b). TEM images of o/w emulsion (5% w/w of oil phase, 10% w/w of  $S_{mix}$  and 85% w/w of water) (c) and nanoemulsion formed after its dilution in a ratio of 1: 100 v/v (d).

(133.27 nm) which may be the result of stronger hydrophobic interactions (Table 2). Polydispersity indicates the uniformity of droplet size within the tested formulation with value ranges from 0.0 to 1.0. The higher the polydispersity, the lower the uniformity of the droplet size. Therefore, by analyzing the PDI values for these nanoformulations we can conclude that they are homogeneous. Also, the Zeta potential value, a measure of the electrostatic repulsion of the droplets, is higher in the case of 3-NE (- 25.33 mV), suggesting good stability during storage.

Next, we evaluated the stability of NE and 3-NE via analysis of particle size and PDI during storage at 4 °C at intervals of 7 days, for up to 28 days, and then after 5 months (152 days), as shown in Fig. 4 a and b. After 7 days, the particle size of NE increased from 133.27 to 149.20 nm, but only small changes were observed subsequent to this. In the case of 3-NE, after recording a decrease in droplet diameter during the first 7 days of study, there were negligible changes in size subsequent to this (Fig. 4 a). PDI, another parameter that was analyzed during the study, was in the range of approximately 0.2 or below during first 28 days for all samples and slightly increased as recorded after 152 days (Fig. 4 b), testifying to the homogeneity of the samples. It is also worth noting that

**Table 2**  
Characterization of unloaded and 3-loaded nanoemulsions.

Code	Diameter (nm)	PdI	Zeta potential (mV)
NE	133.27 ± 1.50	0.172 ± 0.016	- 19.97 ± 0.43
3-NE	117.70 ± 1.08	0.186 ± 0.006	- 25.33 ± 1.59

NE - unloaded nanoemulsion; 3-NE - 3-loaded nanoemulsion (0.02 mg/ml); PDI, polydispersity index.

unimodal size distribution for the 3-encapsulated nanoemulsion was preserved throughout the test period, as shown in Fig. 4 c. Another interesting observation is the fact that, during this experiment, no precipitation of the encapsulated 3 was observed, as is sometimes the case with high dilutions of other formulations with water. Thus, the results clearly confirm the overall stability of the tested nanoemulsions.

With the physicochemical results in hand, we further investigated the cytotoxicity effects of the developed nanoemulsions at two different incubation times, namely 24 and 48 h, using the MTT assay. It is worth highlighting that this issue is particularly important, because some aqueous nanoformulations can be potentially hazardous. To monitor the response of host human cells, we analyzed the effect of NE, 3-NE as well as free 3 on the viability of NHDF cells. We chose this cell line because it has already been established as an *in vitro* model for human cell cytotoxicity of antimalarials, or their formulations, by many other authors [77–81]. The scientific literature also provides examples of the use of fibroblasts as exemplary control lines representing healthy cells, or to demonstrate selectivity for various types of compounds or formulations [82–84]. As we previously demonstrated, free 3, with an  $IC_{50}$  32043.3 ± 1429.5 ng/ml determined for the NHDF cell-line (Table 1), has negligible effect on cell viability at the tested concentration range. Moreover, these mammalian cells were tolerant to 3 encapsulated in a nanoemulsion and no significant changes in cell viability were observed, even at a concentration corresponding to twice the value of the  $IC_{50}$  determined for *P. falciparum* (Fig. 5 a and b).

Bearing in mind the fact that this formulation will be administered orally, we additionally used an *in vitro* model for intestinal cells, namely

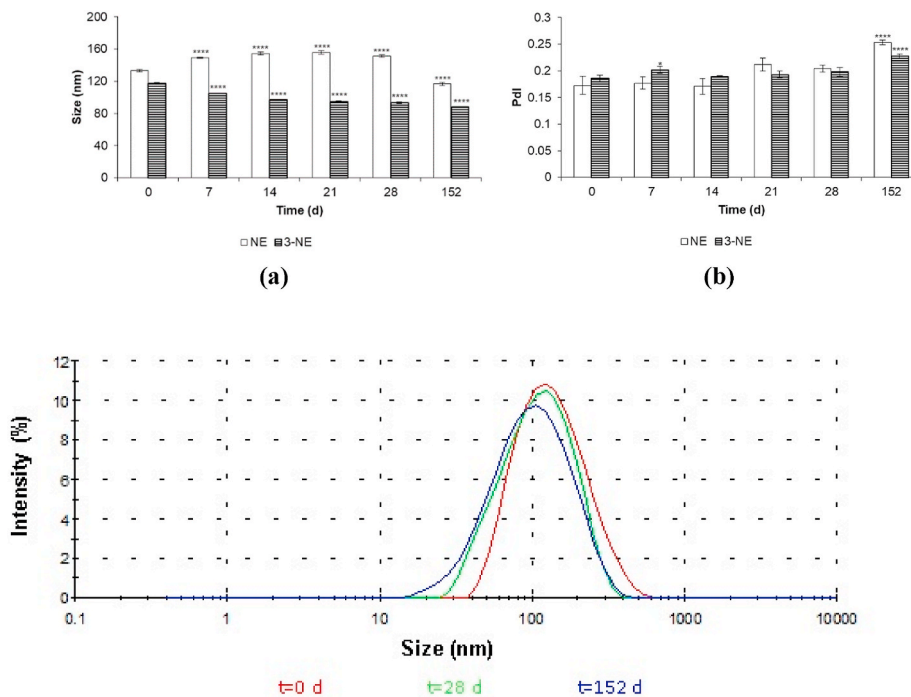


**Fig. 4.** Changes in size (a) and PDI (b) of NE and 3-NE during a 152-day period on storage at 4 °C. Size distributions of 3-NE just after preparation (t = 0), after 28 days (t = 28) and after 152-days of storage (t = 152) (c). \* show the statistical significance calculated with One-way ANOVA (\*p < 0.05 and \*\*\*\* p < 0.0001) as compared to t = 0 d.

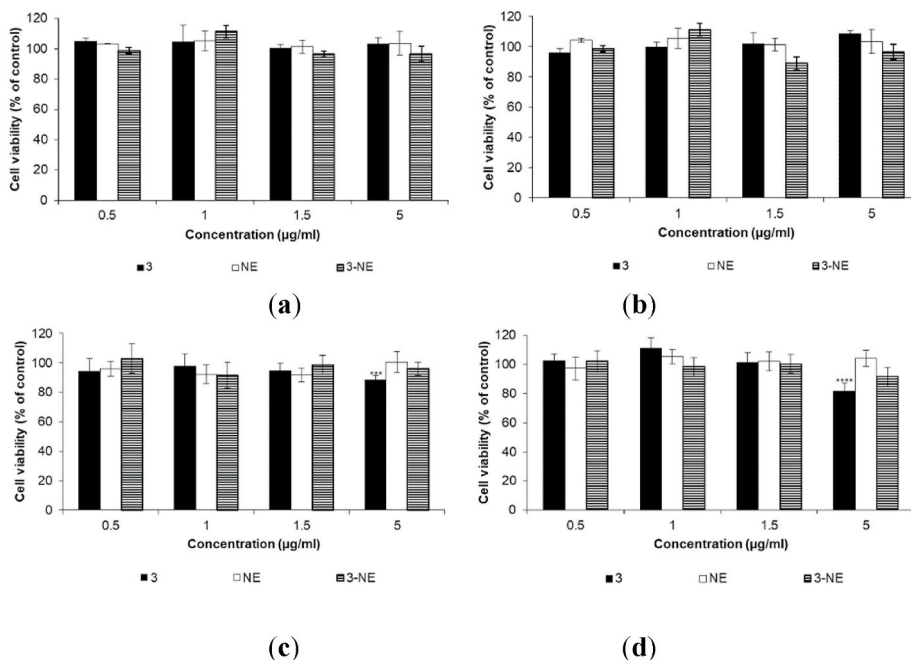


**Fig. 5.** Cytotoxicity studies of 3, in free form and encapsulated in 3-NE, on NHDF cells for 24 h (a) or 48 h (b) and on Caco-2 cells for 24 h (c) or 48 h (d). NE was applied at the same amount as 3-NE. \* show the statistical significance calculated with One-way ANOVA (\*\*\*p < 0.001 and \*\*\*\*p < 0.0001), as compared to control (not treated cells).

the Caco-2 cell-line. This particular cell-line is widely used for the determination of toxicological effects on the gastrointestinal system. As shown in Fig. 5 c and d, cell viabilities were higher than 80% when exposed to the same treatments as used for human fibroblasts. This indicates that the applied samples at the concentrations we used were non-toxic to Caco-2 cells.

Knowing that this particular cell-line is also used for determining

intestinal drug absorption and for assessing the bioavailability of both drugs and their formulations [85,86], we expanded our research to include an uptake study using these cells. Efficient cellular uptake within cells is crucial for the success of nanoformulations, as is the case for oral drug delivery systems. Therefore, to visualize this process, we labeled the oil phase of NE with Nile Red, a fluorescent probe frequently used for labeling lipid dispersions [87]. Confocal microscopic imaging of



Caco-2 cells after 4 h incubation with Nile Red loaded nanoemulsion at 37 °C is shown in Fig. 6. As can be seen, fluorescent signals (red fluorescence) were observed after such treatment, constituting proof that internalization of Nile Red-NE occurred, with most cells demonstrating a cytoplasmic localization of the dye. Cytoplasmic localization was further confirmed by digital imaging of the fluorescence signal from the dye and images of the cells observed under transmitted light (data not shown). This is in accordance with the published work by Fan et al. [88] showing that corn oil nanoemulsions (with sizes of 170, 265 and 556 nm) with incorporated Nile Red were absorbed by Caco-2 cells, demonstrating simultaneously a positive correlation between reduced droplet size and increased cellular uptake. Also, as established previously for nutraceutical beta-carotene nanoemulsions, smaller droplet size has been shown to correlate with improved bioaccessibility [89].

The plots of mean plasma concentrations versus time for **3** in the form of **3-NE** after *i.g.* gavage are depicted in Fig. 7. The pharmacokinetic parameters calculated by a non-compartmental approach are given in Table 3. The compound was eliminated relatively quickly from the mouse body. After *i.g.* administration of **3** in the form of **3-NE** (0.02 mg/ml), the terminal half-life was 70 min. The compound has a large apparent volume of distribution (19.73 L/kg) that indicates the ability for penetration to the deep compartments. After *i.g.* administration, **3** quickly reaches a maximum concentration in the blood ( $C_{max} = 4.67$  ng/ml) within 5 min.

One of the purposes of this study was to investigate the pharmacokinetic profile of compound **3** after its *i.g.* administration in mice at a dose of 0.02 mg/kg in **3-NE**. The concentration of target compound in plasma was determined by LC/ESI-MS/MS. Concentrations of compound **3** in **3-NE** were detectable for at least 8 h after administration. The pharmacokinetic results demonstrated that the absorption of **3** in the form of **3-NE** was rapid, with the peak concentration occurring 5 min after *i.g.* administration.

A critical question to be addressed is whether **3** encapsulated in **3-NE** still possess antimalarial properties and is able to inhibit the growth of both strains of parasite. Analysis of the data shown in Fig. 8 allowed several important observations. The first remark is that, after addition of **3-NE**, significant reduction of growth of *P. falciparum* was observed for both CQ-sensitive and CQ-resistant strains of the parasite. This inhibition, expressed by the value of  $IC_{50}$ , is 2.8 (D10) and 4.2 (W2) times smaller, respectively, compared to that of the free form **3**. These data are very encouraging, due to the fact that, in some cases, encapsulation of the antimalarial compound does not result in a reduction of the  $IC_{50}$ . This phenomenon was described by Melariri et al. after administration of tafenoquine in a microemulsion formulation [90]. Another important observation is the fact that the empty NE nanoemulsion carrier also exhibited significant antimalarial activity, which is a very interesting phenomenon. This may be a consequence of the specific composition of the oil phase, because, as established by Carballeira et al. [91], different fatty acids were proved to act as antimalarial agents. As described by Kumaratilake et al. [92], n-3 and n-6 polyunsaturated fatty acids were also found to possess antimalarial activities. Moreover, this study also showed that the methyl ester of the 22:6 (n-3) fatty acid was as active as the free acid in killing intraerythrocytic forms of the *Plasmodium*. Thus,

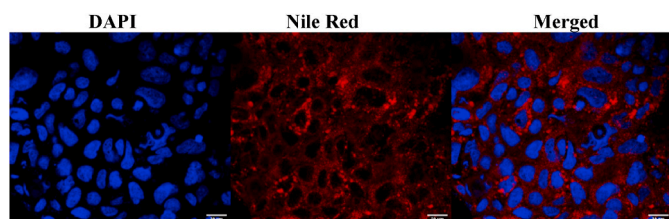


Fig. 6. Confocal microscopy images of Caco-2 cells treated with Nile Red loaded NE for 4 h. Cell nuclei were stained with DAPI (blue), NE uptake was visualized by Nile Red fluorescence (red).

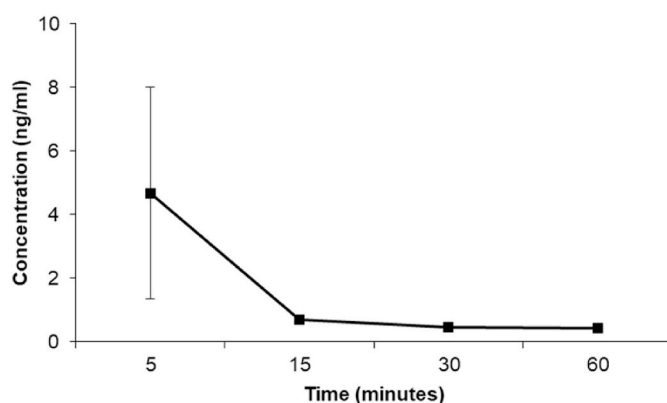


Fig. 7. Concentration – time profiles for **3** in plasma after intragastric gavage to mice at a dose of 0.02 mg/kg in **3-NE** (linear plots).

Table 3  
Pharmacokinetic parameters for **3** after *i.g.* administration at a dose of 0.02 mg/kg in **3-NE** to mice.

PK parameters	
AUC <sub>0-t</sub> [ng · min/ml]	60.13
$\lambda_z$ [min <sup>-1</sup> ]	0.0099
t <sub>0.5</sub> [min]	70.33
MRT [min]	76.67
C <sub>max</sub> [ng/ml]	4.67
t <sub>max</sub> [min]	5.0
V <sub>d</sub> /F [L/kg]	19.73
Cl/F [L/min/kg]	0.194

AUC<sub>0-t</sub> - area under the curve from zero to the last sampling time;  $\lambda_z$  - elimination rate constant; t<sub>0.5</sub> - terminal half life; C<sub>max</sub> - maximum plasma concentration; t<sub>max</sub> - time to reach C<sub>max</sub>; V<sub>d</sub>/F - apparent volume of distribution; Cl/F - apparent clearance; MRT - mean residence time.

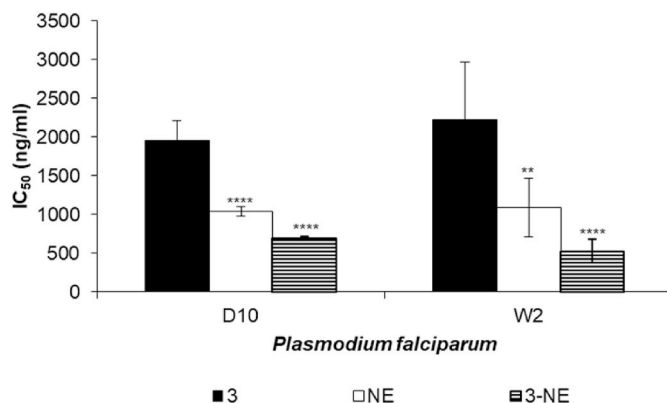


Fig. 8. Inhibition of growth of *P. falciparum* D10 and W2 strains *in vitro* after treatment with NE and **3-NE**. Data for **3** from Table 1. \* show the statistical significance (\*\*p < 0.01 and \*\*\*\*p < 0.0001) as compared to free **3** treated) calculated with One-way ANOVA.

our results indicate that ethyl esters of polyunsaturated acids may also exhibit such properties.

It is also evident from others reports that nanoencapsulation of antimalarial drugs lead to an increase in their bioavailability. For example, Ghosh et al. described that nanotized curcumin was found to be ten-fold more effective for growth inhibition of the *P. falciparum* 3D7 chloroquine sensitive strain *in vitro*, as compared to native curcumin [74]. Although the  $IC_{50}$  reduction obtained by us is not as great as in the case mentioned above, an interesting observation is the fact that **3-NE** is more active against the CQ resistant strain. This is an extremely

important observation, especially in view of the common resistance of parasites to CQ, which is why this issue will be the subject of our further research.

#### 4. Conclusions

In the present study, a novel o/w nanoemulsion formulation with ethyl esters of n-3 and n-6 polyunsaturated fatty acids as oil phase was developed to enhance efficacy of **3**, the most active representative of the series of studied azacarbazoles. The results of this study provide evidence that **3-NE** had enhanced *in vitro* antiplasmodial activities against both CQ-sensitive and CQ-resistant strains of *P. falciparum*, but no cytotoxic effects against mammalian cell lines and demonstrated rapid absorption after intragastric administration. Therefore, adaptation of this nanoencapsulation approach could be considered as a promising delivery system of active agents for treating malaria or other infectious diseases.

#### Authorship contribution statement

Conceptualization, A.J.; formal analysis, A.J., S.P., N.B., M.Z.C., A.Z., M.W. B.T. and Ł.K.; investigation, A.J., S.P., N.B., M.Z.C., A.L., A.Z., M. W. and Ł.K.; resources, A.J., S.P., N.B., M.Z.C., A.Z., M.W., M.Ł., Ł.K. and J.G.; writing—original draft preparation, A.J., M.Z.C., A.Z. and M. W.; writing—review and editing, A.J., S.P., N.B., M.Z.C., A.L., A.Z., M. W., B.T., M.Ł., Ł.K. and J.G.; visualization, A.J., M.Z.C., A.L., A.G. and J. G.; supervision, A.J.; project administration, A.J.; funding acquisition, A.J. and J.G. All authors have read and agreed to the published version of the manuscript.

#### Funding

This work was funded by the statutory activity of subsidy from the Polish Ministry of Science and Higher Education for the Faculty of Biotechnology and Faculty of Chemistry of the University of Wrocław and by Ministero dell'Istruzione, dell'Università e della Ricerca [PRIN 2015.4JRJPP\_004]. Publication costs were supported by Wrocław Center of Biotechnology program “The Leading National Research Center (KNOW) for years 2014–2018”.

#### Declaration of competing interest

None.

#### References

- [1] WHO World Malaria Report 2019, World Health Organization, Geneva, 2019, 978-92-4-156572-1. Licence: CC BY-NC-SA 3.0 IGO.
- [2] I. Petersen, R. Eastman, M. Lanzer, Drug-resistant malaria: molecular mechanisms and implications for public health, *FEBS Lett.* 585 (2011) 1551–1562, <https://doi.org/10.1016/j.febslet.2011.04.042>.
- [3] P.D. Roepe, Molecular and physiologic basis of quinoline drug resistance in *Plasmodium falciparum* malaria, *Future Microbiol.* 4 (2009) 441–455, <https://doi.org/10.2217/fmb.09.15>.
- [4] WHO Eliminating Malaria: Learning from the Past, Looking Ahead, World Health Organization, Geneva, 2011, ISBN 978-92-4-150250-4.
- [5] R.M. Fairhurst, A.M. Dondorp, Artemisinin-Resistant *Plasmodium falciparum* malaria, *Microbiol. Spectr.* 4 (2016) 1–16.
- [6] A.M. Dondorp, F. Nosten, P. Yi, D. Das, A.P. Phyo, J. Tarning, K.M. Lwin, F. Ariey, W. Hanpithakpong, S.J. Lee, P. Ringwald, K. Silamut, M. Imwong, K. Chotivanich, P. Lim, T. Herdman, S.S. An, S. Yeung, P. Singhasivanon, N.P. Day, N. Lindegardh, D. Socheat, N.J. White, Artemisinin resistance in *Plasmodium falciparum* malaria, *N. Engl. J. Med.* 361 (2009) 455–467, <https://doi.org/10.1056/NEJMoa0808859>.
- [7] E.A. Ashley, M. Dhorda, R.M. Fairhurst, C. Amaratunga, P. Lim, S. Suon, S. Sreng, J. M. Anderson, S. Mao, B. Sam, Ch Sopha, C.M. Chhuor, C. Nguon, S. Sovannaroeth, S. Pukrittayakamee, P. Jittamala, K. Chotivanich, K. Chutasmit, C. Suchatsoonthorn, R. Runcharoen, T.T. Hien, N.T. Thuy-Nhien, N.V. Thanh, N. H. Phu, Y. Htut, K.T. Han, K.H. Aye, O.A. Mokuolu, R.R. Olaosebikan, O. O. Folaranmi, M. Mayxay, M. Khantavong, B. Hongvanthong, P.N. Newton, M. A. Onyamboko, C.I. Fanello, A.K. Tshetu, N. Mishra, N. Valecha, A.P. Phyo, F. Nosten, P. Yi, R. Tripura, S. Borrmann, M. Bashraheil, J. Peshu, M.A. Faiz, A. Ghose, M.A. Hossain, R. Samad, M.R. Rahman, M.M. Hasan, A. Islam, O. Miotto,

- R. Amato, B. MacInnis, J. Stalker, D.P. Kwiatkowski, Z. Bozdech, A. Jeeyapant, P. Y. Cheah, T. Sakulthaew, J. Chalk, B. Intharabut, K. Silamut, S.J. Lee, B. Vihokhern, Ch Kunasol, M. Imwong, J. Tarning, W.J. Taylor, S. Yeung, Ch J. Woodrow, J. A. Flegg, D. Das, J. Smith, M. Venkatesan, Ch.V. Plowe, K. Stepniewska, P.J. Guerin, A.M. Dondorp, N.P. Day, N.J. White, Spread of artemisinin resistance in *Plasmodium falciparum* malaria, *N. Engl. J. Med.* 371 (2014) 411–423, <https://doi.org/10.1056/NEJMoa1314981>.
- [8] J.E. Hyde, Drug - resistant malaria - an insight, *FEBS J.* 274 (2007) 4688–4698, <https://doi.org/10.1111/j.1742-4658.2007.05999.x>.
- [9] R.G. Ridley, Medical need, scientific opportunity and the drive for antimalarial drugs, *Nature* 415 (2002) 686–693, <https://doi.org/10.1038/415686a>.
- [10] N.S. Santos-Magalhães, V.C. Mosqueira, Nanotechnology applied to the treatment of malaria, *Adv. Drug Deliv. Rev.* 62 (2010) 560–575, <https://doi.org/10.1016/j.addr.2009.11.024>.
- [11] N.P. Aditya, P.G. Vathsala, V. Vieira, R.S. Murthy, E.B. Souto, Advances in nanomedicine for malaria treatment, *Adv. Colloid Interface Sci.* 201–202 (2013) 1–17, <https://doi.org/10.1016/j.cis.2013.10.014>.
- [12] N. Puttappa, R.S. Kumar, G. Kuppusamy, A. Radhakrishnan, Nano-facilitated drug delivery strategies in the treatment of plasmodium infection, *Acta Trop.* 195 (2019) 103–114, <https://doi.org/10.1016/j.actatropica.2019.04.020>.
- [13] N.P. Aditya, G. Chimote, K. Gunalan, R. Banerjee, S. Patankar, B. Madhusudhan, Curcuminoids-loaded liposomes in combination with artemether protects against *Plasmodium berghei* infection in mice, *Exp. Parasitol.* 131 (2012) 292–299, <https://doi.org/10.1016/j.exppara.2012.04.010>.
- [14] B. Isacchi, M.C. Bergonzi, M. Grazioso, C. Righeschi, A. Pietretti, C. Severini, A. R. Bilia, Artemisinin and artemisinin plus curcumin liposomal formulations: enhanced antimalarial efficacy against *Plasmodium berghei*-infected mice, *Eur. J. Pharm. Biopharm.* 80 (2012) 528–534, <https://doi.org/10.1016/j.ejpb.2011.11.015>.
- [15] V. Rajendran, S. Rohra, M. Raza, G.M. Hasan, S. Dutt, P.C. Ghosh, Stearylamine liposomal delivery of monensin in combination with free artemisinin eliminates blood stages of *Plasmodium falciparum* in culture and *P. berghei* infection in murine malaria, *Antimicrob. Agents Chemother.* 60 (2016) 1304–1318, <https://doi.org/10.1128/AAC.01796-15>.
- [16] W.N. Omwoyo, B.O. Ogutu, F. Oloo, H. Swai, L. Kalombo, P. Melariri, G. M. Mahanga, J.W. Gathirwa, Preparation, characterization, and optimization of primaquine-loaded solid lipid nanoparticles, *Int. J. Nanomed.* 9 (2014) 3865–3874, <https://doi.org/10.2147/IJN.S62630>.
- [17] J.O. Muga, J.W. Gathirwa, M. Tukulula, W.G.Z.O. Jura, In vitro evaluation of chloroquine-loaded and heparin surface-functionalized solid lipid nanoparticles, *Malar. J.* 17 (2018) 2–7, <https://doi.org/10.1186/s12936-018-2302-9>.
- [18] P. Melariri, L. Kalombo, P. Nkuna, A. Dube, R. Hayeshi, B. Ogutu, L. Gibbard, C. deKock, P. Smith, L. Wiesner, H. Swai, Oral lipid-based nanoformulation of tafenoquine enhanced bioavailability and blood stage antimalarial efficacy and led to a reduction in human red blood cell loss in mice, *Int. J. Nanomed.* 10 (2015) 1493–1503, <https://doi.org/10.2147/IJN.S76317>.
- [19] M. Joshi, S. Pathak, S. Sharma, V. Patravale, Solid microemulsion concentrate (NanOsorb) of artemether for effective treatment of malaria, *Int. J. Pharm.* 362 (2008) 172–178, <https://doi.org/10.1016/j.ijpharm.2008.06.012>.
- [20] S.D. Mandawgade, S. Sharma, V.B. Pathak, Development of SMEDDS using natural lipophile: application to beta-Artemether delivery, *Int. J. Pharm.* 362 (2008) 179–183, <https://doi.org/10.1016/j.ijpharm.2008.06.021>.
- [21] C. Solans, P. Izquierdo, J. Nolla, N. Azemar, M.J. Garcia-Celma, Nano-emulsions, *Curr. Opin. Colloid Interface Sci.* 10 (2005) 102–110, <https://doi.org/10.1016/j.cocis.2005.06.004>.
- [22] R. Savla, J. Browne, V. Plassat, K.M. Wasan, E.K. Wasan, Review and analysis of FDA approved drugs using lipid-based formulations, *Drug Dev. Ind. Pharm.* 43 (2017) 1743–1758, <https://doi.org/10.1080/03639045.2017.1342654>.
- [23] K.K. Singh, S.K. Vingkar, Formulation, antimalarial activity and biodistribution of oral lipid nanoemulsion of primaquine, *Int. J. Pharm.* 347 (2008) 136–143, <https://doi.org/10.1016/j.ijpharm.2007.06.035>.
- [24] M. Laxmi, A. Bhardwaj, S. Mehta, A. Mehta, Development and characterization of nanoemulsion as carrier for the enhancement of bioavailability of artemether, *Artif Cells Nanomed. Biotechnol.* 43 (2015) 334–344, <https://doi.org/10.3109/21691401.2014.887018>.
- [25] V. Borhade, S. Pathak, S. Sharma, V. Patravale, Clotrimazole nanoemulsion for malaria chemotherapy. Part II: stability assessment, *in vivo* pharmacodynamic evaluations and toxicological studies, *Int. J. Pharm.* 431 (2012) 149–160, <https://doi.org/10.1016/j.ijpharm.2011.12.031>.
- [26] H.J. Knölker, K.R. Reddy, Isolation and synthesis of biologically active carbazole alkaloids, *Chem. Rev.* 102 (2002) 4303–4427, <https://doi.org/10.1021/cr200059j>.
- [27] A.W. Schmidt, K.R. Reddy, H.J. Knölker, Occurrence, biogenesis, and synthesis of biologically active carbazole alkaloids, *Chem. Rev.* 112 (2012) 3193–3328, <https://doi.org/10.1021/cr200447s>.
- [28] A. Gluszyńska, Biological potential of carbazole derivatives, *Eur. J. Med. Chem.* 94 (2015) 405–426, <https://doi.org/10.1016/j.ejmech.2015.02.059>.
- [29] W. Wang, Q. Li, Y. Wei, J. Xue, X. Sun, Y. Yu, Z. Chen, S. Li, L. Duan, Novel carbazole aminoalcohols as inhibitors of  $\beta$ -hematin formation: antiplasmodial and antischistosomal activities, *Int. J. Parasitol. Drugs Drug Resist.* 7 (2017) 191–199, <https://doi.org/10.1016/j.ijpddr.2017.03.007>.
- [30] T. Wang, P. Mäser, D. Picard, Inhibition of *Plasmodium falciparum* Hsp90 contributes to the antimalarial activities of aminoalcohol-carbazoles, *J. Med. Chem.* 59 (2016) 6344–6352, <https://doi.org/10.1021/acs.jmedchem.6b00591>.
- [31] J. Molette, J. Routier, N. Abla, D. Besson, A. Bombrun, R. Brun, H. Burt, K. Georgi, M. Kaiser, S. Nwaka, M. Muzerelle, A. Scheer, Identification and optimization of an

- aminoalcohol-carbazole series with antimalarial properties, *ACS Med. Chem. Lett.* 4 (2013) 1037–1041, <https://doi.org/10.1021/ml400015f>.
- [32] P.Y. Wang, H.S. Fang, W.B. Shao, J. Zhou, Z. Chen, B.A. Song, S. Yang, Synthesis and biological evaluation of pyridinium-functionalized carbazole derivatives as promising antibacterial agents, *Bioorg. Med. Chem. Lett.* 27 (2017) 4294–4297, <https://doi.org/10.1016/j.bmcl.2017.08.040>.
- [33] A. Caruso, J. Ceramella, D. Iacopetta, C. Saturnino, M.V. Mauro, R. Bruno, S. Aquaro, M.S. Sinicropi, Carbazole derivatives as antiviral agents: an overview, *Molecules* 24 (2019) 1–23, <https://doi.org/10.3390/molecules24101912>.
- [34] Y. Zhang, V.K.R. Tangadanchu, R.R.Y. Bheemanaboina, Y. Cheng, C.H. Zhou, Novel carbazole-triazole conjugates as DNA-targeting membrane active potentiators against clinical isolated fungi, *Eur. J. Med. Chem.* 155 (2018) 579–589, <https://doi.org/10.1016/j.ejmech.2018.06.022>.
- [35] W. Wang, J. Li, J. Yao, T. Wang, S. Li, X. Zheng, I. Duan, W. Zhang, In vitro and in vivo efficacies of novel carbazole aminoalcohols in the treatment of cystic echinococcosis, *J. Antimicrob. Chemother.* 72 (2017) 3122–3130, <https://doi.org/10.1093/jac/dkx250>.
- [36] H. De Jesus-Cortes, P. Xu, J. Drawbridge, S.J. Estill, P. Huntington, S. Tran, J. Britt, R. Tesla, L. Morlock, J. Naidoo, L.M. Melito, G. Wang, N.S. Williams, J.M. Ready, S. L. McKnight, A.A. Pieper, Neuroprotective efficacy of aminopropyl carbazoles in a mouse model of Parkinson disease, *Proc. Natl. Acad. Sci. U.S.A.* 109 (2012) 17010–17015, <https://doi.org/10.1073/pnas.1213956109>.
- [37] H.J. Yoon, S.Y. Kong, M.H. Park, Y. Cho, S.E. Kim, J.Y. Shin, S.H. Jung, J. Lee, Farhanullah, H.J. Kim, J. Lee, Aminopropyl carbazole analogues as potent enhancers of neurogenesis, *Bioorg. Med. Chem. Lett.* 21 (2013) 7165–7174, <https://doi.org/10.1016/j.bmcl.2013.08.066>.
- [38] A.A. Pieper, S.L. McKnight, J.M. Ready, P7C3 and an unbiased approach to drug discovery for neurodegenerative diseases, *Chem. Soc. Rev.* 43 (2014) 6716–6726, <https://doi.org/10.1039/c3cs60448a>.
- [39] C. Saturnino, D. Iacopetta, M.S. Sinicropi, C. Rosano, A. Caruso, A. Caporale, N. Marra, B. Marengo, M.A. Pronzato, O.I. Parisi, P. Longo, R. Ricciarelli, N-alkyl carbazole derivatives as new tools for Alzheimer's disease: preliminary studies, *Molecules* 19 (2014) 9307–9317, <https://doi.org/10.3390/molecules19079307>.
- [40] A. Caruso, D. Iacopetta, F. Puoci, A.R. Cappello, C. Saturnino, M.S. Sinicropi, Carbazole derivatives: a promising scenario for breast cancer treatment, *Mini Rev. Med. Chem.* 16 (2016) 630–643, <https://doi.org/10.2174/1389557515666150709111342>.
- [41] M.S. Shaikh, R. Karpoomath, N. Thapliyal, R.A. Rane, M.B. Palkar, A.M. Faya, H. M. Patel, W.S. Alwan, K. Jain, G.A. Hampannavar, Current perspective of natural alkaloid carbazole and its derivatives as antitumor agents, *Anticancer Agents Med. Chem.* 15 (2015) 1049–1065, <https://doi.org/10.2174/1871520615666150113105405>.
- [42] L. Stephenson, W.K. Warburton, Synthesis of some substituted  $\alpha$ -carboline, *J. Chem. Soc.* (1970) 1355–1364, <https://doi.org/10.1039/J39700001355>.
- [43] A. Bęalski, Ł. Kaczmarek, P. Nantka-Namirski, Synthesis of carbolines by the Graebe-Ullmann method VI. A novel synthesis of 2-Azacarbazole derivative, *Acta Pol. Pharm.* 41 (1984) 601–606.
- [44] P. Nantka-Namirski, Synthesis of carbolines by the Graebe-Ullmann method. III. Synthesis and inhibiting effect of some derivatives of  $\alpha$ -carboline, *Acta Pol. Pharm.* 19 (1962) 229–242.
- [45] Ł. Kaczmarek, P. Nantka-Namirski, Cancerostatics. IV. On the synthesis of some 1-Azacarbazole derivatives as antineoplastic agents, *Pol. J. Pharmacol. Pharm.* 33 (1981) 121–127.
- [46] P. Nantka-Namirski, Synthesis of some derivatives of  $\alpha$ -carboline, *Acta Pol. Pharm.* 23 (1966) 331–337.
- [47] W. Peczyńska-Czoch, M. Mordarski, Ł. Kaczmarek, P. Nantka-Namirski, Structure-activity relationship studies on selected iso- $\alpha$ -carboline I Arch, *Immunol. Ther. Exp.* 34 (1986) 327–331.
- [48] Ł. Kaczmarek, A. Bęalski, P. Nantka-Namirski, A convenient synthesis of symmetrical diazacarbazoles, *Pol. J. Chem.* (1980) 1585–1590.
- [49] Ł. Kaczmarek, Bipyridines. Part XX. Synthesis and properties of some pyrrolodipyridine anhydronium bases, *Bull. Pol. Acad. Sci.* 35 (1987) 269–277.
- [50] W. Trager, J.B. Jensen, Human malaria parasites in continuous culture, *Science* 193 (1976) 673–675, <https://doi.org/10.1126/science.781840>.
- [51] M.T. Makler, D.J. Hinrichs, Measurement of the lactate dehydrogenase activity of *Plasmodium falciparum* as an assessment of parasitemia, *Am. J. Trop. Med. Hyg.* 48 (1993) 205–210, <https://doi.org/10.4269/ajtmh.1993.48.205>.
- [52] A. Jaromin, R. Zarnowski, M. Piętko-Ottlik, D.R. Andes, J. Gubernator, Topical delivery of ebelen encapsulated in biopolymeric nanocapsules: drug repurposing enhanced antifungal activity, *Nanomedicine* 13 (2018) 1139–1155, <https://doi.org/10.2217/nmm-2017-0337>.
- [53] T. Mosmann, Rapid colorimetric assay for cellular growth and survival: application to proliferation and cytotoxicity assays, *J. Immunol. Methods* 65 (1983) 55–63, [https://doi.org/10.1016/0022-1759\(83\)90303-4](https://doi.org/10.1016/0022-1759(83)90303-4).
- [54] A. Daina, O. Michielin, V. Zoete, SwissADME: a free web tool to evaluate pharmacokinetics, drug-likeness and medicinal chemistry friendliness of small molecules, *Sci. Rep.* 7 (2017) 1–13, <https://doi.org/10.1038/srep42717>.
- [55] F. Omodeo-Sale, L. Cortelezzi, N. Basilio, M. Casagrande, A. Sparatore, D. Taramelli, Novel antimalarial aminoquinolines: heme binding and effects on normal or *Plasmodium falciparum*-parasitized human erythrocytes, *Antimicrob. Agents Chemother.* 53 (2009) 4339–4344, <https://doi.org/10.1128/AAC.00536-09>.
- [56] A. Jaromin, M. Korycińska, M. Piętko-Ottlik, W. Musiał, W. Peczyńska-Czoch, Ł. Kaczmarek, A. Kozubek, Membrane perturbations induced by new analogs of neocryptolepine, *Biol. Pharm. Bull.* 35 (2012) 1432–1439.
- [57] F. Shakeel, S. Baboota, A. Ahuja, J. Ali, M. Aqil, S. Shafiq, Nanoemulsions as vehicles for transdermal delivery of aceclofenac, *AAPS PharmSciTech* 8 (2007) 191, <https://doi.org/10.1208/pt0804104>.
- [58] A.R. Neves, J.F. Queiroz, S.A. Costa Lima, F. Figueiredo, R. Fernandes, S. Reis, Cellular uptake and transcytosis of lipid-based nanoparticles across the intestinal barrier: relevance for oral drug delivery, *J. Colloid Interface Sci.* 463 (2016) 258–265, <https://doi.org/10.1016/j.jcis.2015.10.057>.
- [59] Eur – lex access to European union law. <https://eur-lex.europa.eu/legal-content/EN/TXT/?uri=celex:32010L0063>, 2020. (Accessed 19 May 2020).
- [60] K. Patel, C.M. Kirkpatrick, Pharmacokinetic concepts revisited—basic and applied, *Curr. Pharm. Biotechnol.* 12 (2011) 1983–1990, <https://doi.org/10.2174/138920111798808400>.
- [61] R. Muniguntti, K. Becker, R. Brun, A.I. Calderón, Determination of antiplasmodial activity and binding affinity of selected natural products towards PfTrxR and PfGR, *Nat. Prod. Commun.* 8 (2013) 1135–1136.
- [62] M.A. Rudzinska, W. Trager, R.S. Bray, Pinocytotic uptake and the digestion of hemoglobin in malaria parasites, *J. Protozool.* 12 (1965) 563–576, <https://doi.org/10.1111/j.1550-7408.1965.tb03256.x>.
- [63] A.F. Slater, W.J. Swiggard, B.R. Orton, W.D. Flitter, D.E. Goldberg, A. Cerami, G. B. Henderson, An iron-carboxylate bond links the heme units of malaria pigment, *Proc. Natl. Acad. Sci. U.S.A.* 88 (1991) 325–329, <https://doi.org/10.1073/pnas.88.2.325>.
- [64] T.J. Egan, Recent advances in understanding the mechanism of hemozoin (malaria pigment) formation, *J. Inorg. Biochem.* 102 (2008) 1288–1299, <https://doi.org/10.1016/j.jinorgbio.2007.12.004>.
- [65] C.D. Fitch, Antimalarial schizontocides: ferriprotoporphyrin IX interaction hypothesis, *Parasitol. Today* 2 (1986) 330–331, [https://doi.org/10.1016/0169-4758\(86\)90051-7](https://doi.org/10.1016/0169-4758(86)90051-7).
- [66] D.J. Sullivan Jr., I.Y. Gluzman, D.G. Russell, D.E. Goldberg, On the molecular mechanism of chloroquine's antimalarial action, *Proc. Natl. Acad. Sci. U.S.A.* 93 (1996) 11865–11870, <https://doi.org/10.1073/pnas.93.21.11865>.
- [67] D.J. Schaer, P.W. Buehler, A.I. Alayash, J.D. Belcher, G.M. Vercellotti, Hemolysis and free hemoglobin revisited: exploring hemoglobin and heme scavengers as a novel class of therapeutic proteins, *Blood* 121 (2013) 1276–1284, <https://doi.org/10.1182/blood-2012-11-451229>.
- [68] K. Rehman, F. Lötsch, P.G. Kremsner, M. Ramharter, Haemolysis associated with the treatment of malaria with artemisinin derivatives: a systematic review of current evidence, *Int. J. Infect. Dis.* 29 (2014) 268–273, <https://doi.org/10.1016/j.ijid.2014.09.007>.
- [69] U. Müller-Eberhard, J. Javid, H.H. Liem, A. Hanstein, M. Hanna, Plasma concentrations of hemopexin, haptoglobin and heme in patients with various hemolytic diseases, *Blood* 32 (1968) 811–815.
- [70] A.C. Chou, C.D. Fitch, Hemolysis of mouse erythrocytes by ferriprotoporphyrin IX and chloroquine: chemotherapeutic implications, *J. Clin. Invest.* 66 (1980) 856–858, <https://doi.org/10.1172/JCI109925>.
- [71] H. Ginsburg, R.A. Demel, The effect of ferriprotoporphyrin IX and chloroquine on phospholipid monolayers and the possible implications to antimalarial activity, *Biochim. Biophys. Acta* 732 (1983) 316–319, [https://doi.org/10.1016/0005-2736\(83\)90219-5](https://doi.org/10.1016/0005-2736(83)90219-5).
- [72] A. Sparatore, N. Basilio, S. Parapini, S. Romeo, F. Novelli, F. Sparatore, D. Taramelli, Aminoquinoline quinolizidinyl- and quinolizidinylalkyl-derivatives with antimalarial activity, *Bioorg. Med. Chem.* 13 (2005) 5338–5345, <https://doi.org/10.1016/j.bmc.2005.06.047>.
- [73] B.A. Kerwin, Polysorbates 20 and 80 used in the formulation of protein biotherapeutics: structure and degradation pathways, *J. Pharm. Sci.* 97 (2008) 2924–2935, <https://doi.org/10.1002/jps.21190>.
- [74] D.J. Sullivan Jr., S.C. Gad, M. Julien, A review of the nonclinical safety of Transcutol®, a highly purified form of diethylene glycol monoethyl ether (DEGEE) used as a pharmaceutical excipient, *Food Chem. Toxicol.* 72 (2014) 40–50, <https://doi.org/10.1016/j.fct.2014.06.028>.
- [75] K. Kawakami, T. Yoshikawa, Y. Moroto, E. Kanaoka, K. Takahashi, Y. Nishihara, K. Masuda, Microemulsion formulation for enhanced absorption of poorly soluble drugs. I. Prescription design, *J. Control Release* 81 (2002) 65–74, [https://doi.org/10.1016/s0168-3659\(02\)00049-4](https://doi.org/10.1016/s0168-3659(02)00049-4).
- [76] L. Wang, X. Li, G. Zhang, J. Dong, J. Eastoe, Oil-in-water nanoemulsions for pesticide formulations, *J. Colloid Interface Sci.* 314 (2007) 230–235, <https://doi.org/10.1016/j.jcis.2007.04.079>.
- [77] S.O. Sarr, S. Perrotey, I. Fall, S. Ennahar, M. Zhao, Y.M. Diop, E. Candolfi, E. Marchioni, *Icacina senegalensis* (Icacinaeaceae), traditionally used for the treatment of malaria, inhibits in vitro *Plasmodium falciparum* growth without host cell toxicity, *Malar. J.* 10 (2011) 1–10, <https://doi.org/10.1186/1475-2875-10-85>.
- [78] L.F. Silva, E.S. Lima, M.C. Vasconcelos, E.S. Aranha, D.S. Costa, E.V. Mustafa, S. K. Morais, Md Alecrim, S.M. Nunomura, L. Struwe, V.F. de Andrade-Neto, A. M. Pohlit, In vitro and in vivo antimalarial activity and cytotoxicity of extracts, fractions and a substance isolated from the Amazonian plant *Tachia grandiflora* (Gentianaceae), *Mem. Inst. Oswaldo Cruz* 108 (2013) 501–507, <https://doi.org/10.1590/S0074-02762013000400017>.
- [79] A. Ghosh, T. Banerjee, S. Bhandary, A. Suroliya, Formulation of nanotized curcumin and demonstration of its antimalarial efficacy, *Int. J. Nanomedicine* 9 (2014) 5373–5387, <https://doi.org/10.2147/IJN.S62756>.
- [80] M.L. Booker, C.M. Bastos, M.L. Kramer, R.H. Barker Jr., R. Skerlj, A.B. Sidhu, X. Deng, C. Celatka, J.F. Cortese, J.E. Guerrero Bravo, K.N. Crespo Lladod, A. E. Serrano, I. Angulo-Barturen, M.B. Jiménez-Díaz, S. Viera, H. Garutie, S. Wittlin, P. Papastogiannidis, J. Linh, Ch.J. Jansch, S.M. Khanh, M. Duraisinghi, B. Coleman, E.J. Goldsmith, M.A. Phillip, B. Munozb, D. F. Wirthi, J.D. Klinger, R. Wiegand, E. Sybertza, Novel inhibitors of *Plasmodium falciparum* dihydroorotate

- dehydrogenase with anti-malarial activity in the mouse model, *J. Biol. Chem.* 285 (2010) 33054–33364, <https://doi.org/10.1074/jbc.M110.162081>.
- [81] C. Rusconi, N. Vaiana, M. Casagrande, N. Basilio, S. Parapini, D. Taramelli, S. Romeo, A. Sparatore, Synthesis and comparison of antiplasmodial activity of (+), (-) and racemic 7-chloro-4-(N-lupinyl) aminoquinoline, *Bioorg. Med. Chem.* 20 (2012) 5980–5985, <https://doi.org/10.1016/j.bmc.2012.07.041>.
- [82] N. Pravin, G. Kumaravel, R. Senthilkumar, R. Natarajan, Water-soluble Schiff base Cu(II) and Zn(II) complexes: synthesis, DNA targeting ability and chemotherapeutic potential of Cu(II) complex for hepatocellular carcinoma – in vitro and in vivo approach, *Appl Organometal. Chem.* e3739 (2017), <https://doi.org/10.1002/aoc.3739>.
- [83] R. Vecchione, V. Quagliariello, D. Calabria, V. Calcagno, E. De Luca, R. V Iaffaioli, P.A. Netti, Curcumin bioavailability from oil in water nano-emulsions: in vitro and in vivo study on the dimensional, compositional and interactional dependence, *J. Control Release* 233 (2016) 88–100, <https://doi.org/10.1016/j.jconrel.2016.05.004>.
- [84] H. Rachmawati, M.A. Novel, S. Ayu, B. Guntur, O.M. Tandrasasmita, R. R. Tjandrawinata, K. Anggadiredja, The in vitro-in vivo safety confirmation of PEG-40 hydrogenated Castor oil as a surfactant for oral nanoemulsion formulation, *Sci. Pharm.* 85 (2017) 18, <https://doi.org/10.3390/scipharm85020018>.
- [85] Y. Sambuy, I. De Angelis, G. Ranaldi, M.I. Scarino, A. Stammati, F. Zucco, The Caco-2 cell line as a model of the intestinal barrier: influence of cell and culture-related factors on Caco-2 cell functional characteristics, *Cell Biol. Toxicol.* 21 (2005) 1–26, <https://doi.org/10.1007/s10565-005-0085-6>.
- [86] P. Shah, V. Jogani, T. Bagchi, A. Misra, Role of Caco-2 cell monolayers in prediction of intestinal drug absorption, *Biotechnol. Prog.* 22 (2006) 186–198, <https://doi.org/10.1021/bp050208u>.
- [87] P. Greenspan, E.P. Mayer, S.D. Fowler, Nile red: a selective fluorescent stain for intracellular lipid droplets, *J. Cell Biol.* 100 (1985) 965–973, <https://doi.org/10.1083/jcb.100.3.965>.
- [88] Y. Fan, Y. Zhang, W. Yokoyama, J. Yi, Endocytosis of corn oil-caseinate emulsions in vitro: impacts of droplet sizes, *Nanomaterials* 7 (2017) 1–15, <https://doi.org/10.3390/nano7110349>.
- [89] J. Yi, Y. Li, F. Zhong, W. Yokoyama, The physicochemical stability and in vitro bioaccessibility of beta-carotene in oil-in-water sodium caseinate emulsions, *Food Hydrocoll.* 35 (2014) 19–27, <https://doi.org/10.1016/j.foodhyd.2013.07.025>.
- [90] P. Melariri, L. Kalombo, P. Nkuna, A. Dube, R. Hayeshi, B. Ogutu, L. Gibhard, C. deKock, P. Smith, L. Wiesner, Oral lipid-based nanoformulation of tafenoquine enhanced bioavailability and blood stage antimalarial efficacy and led to a reduction in human red blood cell loss in mice, *Int. J. Nanomedicine* 10 (2015) 1493–1503, <https://doi.org/10.2147/IJN.S76317>.
- [91] N. M Carballeira, New advances in fatty acids as antimalarial, antimycobacterial and antifungal agents, *Prog. Lipid Res.* 47 (2008) 50–61, <https://doi.org/10.1016/j.plipres.2007.10.002>.
- [92] L.M. Kumaratilake, B.S. Robinson, A. Ferrante, A. Poulos, Antimalarial properties of n-3 and n-6 polyunsaturated fatty acids: in vitro effects on *Plasmodium falciparum* and in vivo effects on *P. berghei*, *J. Clin. Invest.* 89 (1992) 961–967, <https://doi.org/10.1172/JCI115678>.